Stabilized Nonlocal Model for Dispersive Wave Propagation in Heterogeneous Media

Gakuji Nagai*

Institute of Industrial Science
The University of Tokyo, 4-6-1 Komaba, Meguro, Tokyo 153-8505, Japan
e-mail: gakuji@iis.u-tokyo.ac.jp

Jacob Fish

Department of Civil Engineering
Rensselaer Polytechnic Institute, Troy, NY 12180, USA
e-mail: fishj@rpi.edu

Katsuhiko Watanabe

Institute of Industrial Science
The University of Tokyo, 4-6-1 Komaba, Meguro, Tokyo 153-8505, Japan
e-mail: kwata@iis.u-tokyo.ac.jp

Key words: dispersive wave, heterogeneous media, higher-order homogenization, nonlocal theory, stabilization

Abstract
In this paper, a general-purpose computational model for dispersive wave propagation in heterogeneous media is developed. The model is based on the higher-order homogenization with multiple spatial and temporal scales and the C^0-continuous mixed finite element approximation of the resulting nonlocal equations of motion. The proposed nonlocal Hamilton principle leads to the stable discrete system of equations independent of the mesh size, unit cell domain and the excitation frequency. The method has been validated for plane harmonic analysis and for transient wave motion in semi-infinite domain with various microstructures.

1 Introduction

The primary objective of this paper is to develop a mathematical and computational model for wave propagation in heterogeneous media that would be both stable and accurate for a wide range of wave frequency excitations. It is well known that the $O(1)$ mathematical homogenization123 is valid for the case of the wavelength λ of a traveling wave significantly larger than the characteristic length l of the heterogeneity. However, when the wavelength λ is comparable to that of the characteristic length l, the wave motion is affected by the heterogeneity due to successive reflection and refraction waves from the material interfaces, which is known as the dispersion, polarization correction, and attenuation phenomena at the macro scale 9. For such a case, the higher-order homogenization theory with multiple spatial and temporal scales has been used to resolve dispersion effects 5.

Fish and Chen 4 have shown that the higher-order homogenization with two spatial scales only produces unbounded solution of stress as the time approaches infinity. To alleviate the problem of secularity they introduced multiple slow temporal scales in addition to two spatial scales. One of the solution procedures for the resulting macroscopic equations is based on the nonlocal approach, in which the slow temporal scales can be eliminated. Fish et al.5 have validated this approach in one-dimensional case and for macroscopically isotropic media in multiple dimensions.

In the present paper, we focus on developing a general computational framework for wave propagation in macroscopically anisotropic heterogeneous medium. Attention is restricted to wave motion away from the boundaries.

2 Brief Overview of Previous Work

2.1 Higher-Order Homogenization with Multiple Spatial-Temporal Scales

Assuming that the macroscopic length $L = \lambda / (2\pi)$ is significantly larger than the characteristic length l of the heterogeneity, i.e., $0< l / L = \varepsilon <<1$ 8, consider macro- and micro- coordinate systems $\boldsymbol{x}$ and $\boldsymbol{y}$, respectively, related by

$$\boldsymbol{y}=\boldsymbol{x}/\varepsilon \tag{1}$$

Following 5, in addition to multiple spatial scales the following multiple slow time scales are introduced

$$t_0 = t, \quad t_1 = \varepsilon t, \quad t_2 = \varepsilon^2 t \tag{2}$$

Using the chain rule, the spatial and temporal derivatives can be expressed as

$$\begin{aligned} (\ )_{,i} &= (\ )_{,x_i} + \varepsilon^{-1}(\ )_{,y_i} \\ (\dot{\ }) &= (\ )_{,t_0} + \varepsilon\ (\ )_{,t_1} + \varepsilon^2(\ )_{,t_2} \end{aligned} \tag{3}$$

where the comma followed by the subscript variable denotes the partial derivative and the superscripted dot represents the full time derivative. The displacement field $\boldsymbol{u}$ is approximated using the following asymptotic expansion:

$$u(\boldsymbol{x},\boldsymbol{y},t_0,t_1,t_2) = \boldsymbol{u}^0(\boldsymbol{x},\boldsymbol{y},t_0,t_1,t_2) + \varepsilon\ \boldsymbol{u}^1(\boldsymbol{x},\boldsymbol{y},t_0,t_1,t_2) + \varepsilon^2\boldsymbol{u}^2(\boldsymbol{x},\boldsymbol{y},t_0,t_1,t_2) + \cdots \tag{4}$$

Substituting equation (4) into the governing equation of wave motion and subsequently taking perturbation with respect to ε gives a set of micro and macro equations of motion. Due to the linearity of the micro equations and periodicity, the following decompositions of $\boldsymbol{u}^0$, $\boldsymbol{u}^1$ and $\boldsymbol{u}^2$ are made:

$$\begin{aligned}
&u_i^0(\boldsymbol{x},\boldsymbol{y},t_0,t_1,t_2)=u_i^0(\boldsymbol{x},t_0,t_1,t_2)\\
&u_i^1(\boldsymbol{x},\boldsymbol{y},t_0,t_1,t_2)=U_i^1(\boldsymbol{x},t_0,t_1,t_2)+H_i^{kl}(\boldsymbol{y})\,e_{xkl}(\boldsymbol{u}^0)\\
&u_i^2(\boldsymbol{x},\boldsymbol{y},t_0,t_1,t_2)=U_i^2(\boldsymbol{x},t_0,t_1,t_2)+H_i^{kl}(\boldsymbol{y})\,e_{xkl}(\boldsymbol{U}^1)+P_i^{jkl}(\boldsymbol{y})\big(e_{xkl}(\boldsymbol{u}^0)\big)_{,x_j}
\end{aligned}\tag{5}$$

where $e_{xij}(.)$ denotes the strain operator with respect to the macro-coordinates $\boldsymbol{x}$, and $\boldsymbol{H}$ and $\boldsymbol{P}$ are characteristic functions normalized as:

$$\left\langle H_i^{kl}\right\rangle=0,\qquad \left\langle P_i^{jkl}\right\rangle=0\tag{6}$$

where $\langle\cdot\rangle$ denotes the averaging operator with respect to the micro coordinate $\boldsymbol{y}$. $\boldsymbol{H}$ and $\boldsymbol{P}$ are obtained from the solution of the unit cell (micro) problem subjected to macroscopically constant and linear strain fields, respectively, with periodic boundary conditions. In absence of polarization effect 9, the resulting macroscopic equations of motion up to $O(\varepsilon^2)$ are given as:

$$\begin{aligned}
&O(1):\quad \rho_0 u^0_{i,t_0t_0}-D^0_{ijmn}(e_{xmn}(\boldsymbol{u}^0))_{,x_j}=0\\
&O(\varepsilon^1):\quad \rho_0 U^1_{i,t_0t_0}-D^0_{ijmn}(e_{xmn}(\boldsymbol{U}^1))_{,x_j}=-\left\langle\rho H_i^{kl}\right\rangle(e_{xkl}(\boldsymbol{u}^0))_{,t_0t_0}-2\rho_0u^0_{i,t_0t_1}\\
&O(\varepsilon^2):\quad \rho_0 U^2_{i,t_0t_0}-D^0_{ijmn}(e_{xmn}(\boldsymbol{U}^2))_{,x_j}=D^2_{ijprmn}(e_{xmn}(\boldsymbol{u}^0))_{,x_rx_px_j}-\left\langle\rho H_i^{kl}\right\rangle(e_{xkl}(\boldsymbol{U}^1))_{,t_0t_0}\\
&\quad-\left\langle\rho P_i^{jmn}\right\rangle(e_{xmn}(\boldsymbol{u}^0))_{,x_jt_0t_0}-2\rho_0U^1_{i,t_0t_1}-2\left\langle\rho H_i^{kl}\right\rangle(e_{xkl}(\boldsymbol{u}^0))_{,t_0t_1}-2\rho_0u^0_{i,t_0t_2}-\rho_0u^0_{i,t_1t_1}
\end{aligned}\tag{7}$$

where ρ and $\boldsymbol{D}$ are mass density and elastic tensor, respectively, and

$$\begin{aligned}
&\rho_0=\langle\rho\rangle\\
&D^0_{ijkl}=\left\langle D_{ijmn}\left\{e_{ymn}(\boldsymbol{H}^{kl})+\delta_{mk}\delta_{nl}\right\}\right\rangle\\
&D^2_{ijprkl}=E_{ijpq}D^0_{qrkl}+R_{ijprkl}\\
&E_{ijpq}=\left\langle H_s^{ij}H_s^{pq}\right\rangle\\
&R_{ijprkl}=\Big\langle -H_s^{ij}D_{srtp}H_t^{kl}+e_{ymn}(\boldsymbol{P}^{pij})D_{mnst}e_{yst}(\boldsymbol{P}^{rkl})\\
&\qquad\qquad +H_s^{ij}\big(D_{spmn}e_{ymn}(\boldsymbol{P}^{rkl})-D_{srmn}e_{ymn}(\boldsymbol{P}^{pkl})\big)\Big\rangle
\end{aligned}\tag{8}$$

2.2 Nonlocal Model

To eliminate the multiple temporal scales t_0, t_1, t_2 in equation (7), equation (4) is averaged over the unit cell (micro) domain:

$$\boldsymbol{U}=\langle\boldsymbol{u}\rangle=\boldsymbol{u}^0+\varepsilon\,\boldsymbol{U}^1+\varepsilon^2\boldsymbol{U}^2+\cdots\tag{9}$$

Multiplying the second and the third of equation in (7) by ε and ε^2, respectively, then adding them to the first of it, and finally utilizing the chain rule with respect to the temporal derivative yields

$$\begin{aligned}
&\rho_0\ddot{U}_i-D^0_{ijmn}(e_{xmn}(\boldsymbol{U}))_{,x_j}-\varepsilon^2D^2_{ijprmn}(e_{xmn}(\boldsymbol{U}))_{,x_rx_px_j}\\
&+\varepsilon\left\langle\rho H_i^{mn}\right\rangle e_{xmn}(\ddot{\boldsymbol{U}})+\varepsilon^2\left\langle\rho P_i^{jmn}\right\rangle(e_{xmn}(\ddot{\boldsymbol{U}}))_{,x_j}+O(\varepsilon^3)=0
\end{aligned}\tag{10}$$

Solution of equation (10) by finite element method requires C^1-continuous interpolation due to appearance of the fourth-order spatial derivatives. Furthermore, equation (10) gives rise to the imaginary wave speed for higher wave numbers whose wavelength λ is smaller than the characteristic length l 5. Even though the homogenization theory is not valid for $\lambda < l$, these instabilities may arise when fine meshes are used for the macro problem. In the next section, we present the C^0-continuous finite element formulation with stabilization.

3 Stabilized Nonlocal Modeling

In this section we focus on developing a new mathematical model based on equation (10), which will be stable for all frequency excitations independent of either the unit cell size or the finite element discretization. Moreover, the resulting discrete model will be based on the C^0-continuous finite element formulation.

For simplicity, attention is restricted to constant mass density. In this case, equation (10) can be simplified as follows:

$$\rho_0 \ddot{U}_i - D^0_{ijmn}(e_{xmn}(\boldsymbol{U}))_{,x_j} - \varepsilon^2 D^2_{ijprmn}(e_{xmn}(\boldsymbol{U}))_{,x_r x_p x_j} + O(\varepsilon^3) = 0 \tag{11}$$

Assuming that $e_{xkl}(\boldsymbol{U})_{,x_r x_p}$ is differentiable, only symmetric part of the sixth-order tensor R_{ijprkl} with respect to p and r affects the solution. Thus exploiting this symmetry, $\boldsymbol{R}$ can be rewritten as

$$\begin{aligned} R^s_{ijprkl} &= 1/2\left(R_{ijprkl} + R_{ijrpkl}\right) \\ &= 1/2\left\langle -H^{ij}_s (D_{srtp} + D_{sptr}) H^{kl}_t + \left(e_{ymn}(\boldsymbol{P}^{pij})\, e_{yst}(\boldsymbol{P}^{rkl}) + e_{ymn}(\boldsymbol{P}^{rij})\, e_{yst}(\boldsymbol{P}^{pkl})\right) D_{mnst} \right\rangle \end{aligned} \tag{12}$$

From equation (12) it can be seen that $R_{ijprkl} = R_{klrpij}$. Hence, the symmetric part $\boldsymbol{R}^s$ of $\boldsymbol{R}$ can be recast into the following matrix representation

$$\boldsymbol{R}^s = \left[\begin{array}{cc:cc:cc} R^s_{111111} & & & & & \\ R^s_{112111} & R^s_{112211} & & & \text{Sym.} & \\ \hdashline R^s_{221111} & R^s_{221211} & R^s_{221122} & & & \\ R^s_{221211} & R^s_{222211} & R^s_{221222} & R^s_{222222} & & \\ \hdashline R^s_{121111} & R^s_{121211} & R^s_{121122} & R^s_{121222} & R^s_{121112} & \\ R^s_{121211} & R^s_{122211} & R^s_{121222} & R^s_{122222} & R^s_{121212} & R^s_{122212} \end{array}\right] \tag{13}$$

Using eigen-analysis the matrix $\boldsymbol{R}^s$ can be further decomposed into

$$\boldsymbol{R}^s = \boldsymbol{R}^{s-} + \boldsymbol{R}^{s+} \tag{14}$$

where the eigenvalues of $\boldsymbol{R}^{s-}$ and $\boldsymbol{R}^{s+}$ are semi-negative and semi-positive, respectively. Introducing assumed nonlocal strain $\bar{e}_{ij}$ and assumed nonlocal stress $\bar{\sigma}_{ij}$, the following $O(\varepsilon^2)$ approximation of the nonlocal equation (11) can be obtained.

$$\begin{cases} \rho_0 \ddot{U}_i - \left(\bar{\sigma}_{ij} + \varepsilon^2 \rho_0 E_{ijkl} e_{xkl}(\ddot{\boldsymbol{U}})\right)_{,x_j} = 0 \\ \bar{\sigma}_{ij} = D^0_{ijkl} \bar{e}_{kl} + \varepsilon^2 R^{s-}_{ijprkl} \bar{e}_{kl,x_p x_r} \\ \bar{e}_{ij} = e_{xij}(\boldsymbol{U}) + \varepsilon^2 C^0_{ijmn} R^{s+}_{mnprkl} C^0_{klst} \bar{\sigma}_{st,x_p x_r} \end{cases} \tag{15}$$

where $\boldsymbol{C}^0$ is a compliance of the elastic tensor $\boldsymbol{D}^0$. Note that C^0-continuous finite element interpolation of displacements, assumed stresses and strains can be exercised for the discretization of equation (15). A two-field variational principle was discussed by Peerlings et al.6 in attempt to utilize the C^0-approximation of the nonlocal fields. The two-field approximation is sufficient for stabilization in case

$\boldsymbol{R}^s$ is a positive scalar quantity. However, the three-field approximation is required in case $\boldsymbol{R}^s$ is indefinite.

Remark 1: If $\boldsymbol{R}^{s-}$ and $\boldsymbol{R}^{s+}$ are neglected, the irreducible form of the stabilized equation (15) reduces to:

$$\rho_0 \ddot{U}_i - \left(D^0_{ijkl} e_{xkl}(\boldsymbol{U}) + \varepsilon^2 \rho_0 E_{ijkl} e_{xkl}(\ddot{\boldsymbol{U}})\right)_{,x_j} = 0 \tag{16}$$

This form has been shown to be valid for macroscopically isotropic media 5.

Remark 2: The proof of $O(\varepsilon^2)$ approximation (15) of the nonlocal equation (11) is given below. Assuming that $\bar{e}_{ij,x_r x_p}$ and $\bar{\sigma}_{ij,x_r x_p}$ are differentiable, applying strain operator $e_{xij}(.)$ to the first equation of (15) and multiplying it by ε^2 yields

$$\varepsilon^2 \rho_0 e_{xij}(\ddot{\boldsymbol{U}}) - \frac{\varepsilon^2}{2}\left(\bar{\sigma}_{ir,x_j} + \bar{\sigma}_{jr,x_i}\right)_{,x_r} + O(\varepsilon^4) = 0 \tag{17}$$

Substituting equation (17) into the first equation in (15) we get

$$\rho_0 \ddot{U}_i - \left(\bar{\sigma}_{ij} + \varepsilon^2 E_{ijpq} \bar{\sigma}_{qr,x_p x_r}\right)_{,x_j} + O(\varepsilon^4) = 0 \tag{18}$$

Similarly, substituting the third equation in (15) into the second yields

$$\bar{\sigma}_{ij} = D^0_{ijkl} e_{xkl}(\boldsymbol{U}) + \varepsilon^2 R^{s+}_{ijprkl} C^0_{klst} \bar{\sigma}_{st,x_p x_r} + \varepsilon^2 R^{s-}_{ijprkl} e_{xkl}(\boldsymbol{U})_{,x_p x_r} + O(\varepsilon^4) \tag{19}$$

Taking second-derivative of equation (19) and multiplying it by ε^2 yields

$$\varepsilon^2 \bar{\sigma}_{st,x_p x_r} = \varepsilon^2 D^0_{ijkl} e_{xkl}(\boldsymbol{U})_{,x_p x_r} + O(\varepsilon^4) \tag{20}$$

Substituting equation (20) into (19), we have

$$\bar{\sigma}_{ij} = D^0_{ijkl} e_{xkl}(\boldsymbol{U}) + \varepsilon^2 \left(R^{s+}_{ijprkl} + R^{s-}_{ijprkl}\right) e_{xkl}(\boldsymbol{U})_{,x_p x_r} + O(\varepsilon^4) \tag{21}$$

Finally, substituting equation (21) into (18), we have

$$\rho_0 \ddot{U}_i - D^0_{ijkl} e_{xkl}(\boldsymbol{U})_{,x_j} - \varepsilon^2 \underbrace{\left(E_{ijpq} D^0_{prkl} + R^{s-}_{ijprkl} + R^{s+}_{ijprkl}\right)}_{=D^2_{ijprkl}} e_{xkl}(\boldsymbol{U})_{,x_p x_r x_j} + O(\varepsilon^4) = 0 \tag{22}$$

Remark 3: The corresponding Hamilton principle of equation (15) is given as

$$\int_{T_1}^{T_2} \left[-\delta L(\boldsymbol{U}, \dot{\boldsymbol{U}}, \bar{e}, \bar{\sigma}) - \delta F(\boldsymbol{U}, \dot{\boldsymbol{U}}, \bar{e}, \bar{\sigma})\right] dt = 0 \tag{23}$$

$$\begin{aligned} L(\boldsymbol{U}, \dot{\boldsymbol{U}}, \bar{e}, \bar{\sigma}) = \int_\Omega \Big[& \frac{1}{2}\rho_0 \dot{U}_i \dot{U}_i + \frac{1}{2}\varepsilon^2 \rho_0 E_{ijkl} e_{xij}(\dot{\boldsymbol{U}}) e_{xkl}(\dot{\boldsymbol{U}}) \\ & - \frac{1}{2} D^0_{ijkl} \bar{e}_{ij} \bar{e}_{kl} + \frac{1}{2}\varepsilon^2 R^{s-}_{ijprkl} \bar{e}_{ij,x_p} \bar{e}_{kl,x_r} \\ & + \frac{1}{2}\varepsilon^2 C^0_{ijmn} R^{s+}_{mnprst} C^0_{stkl} \bar{\sigma}_{ij,x_p} \bar{\sigma}_{kl,x_r} \\ & - \bar{\sigma}_{ij}\left(e_{xij}(\boldsymbol{U}) - \bar{e}_{ij}\right)\Big] d\Omega \end{aligned} \tag{24}$$

$$\begin{aligned} \delta F(\boldsymbol{U}, \dot{\boldsymbol{U}}, \bar{e}, \bar{\sigma}) = & \int_{\Gamma_\sigma} \delta U_i \left(f_i + \varepsilon^2 \rho_0 E_{ijkl} e_{xkl}(\ddot{\boldsymbol{U}}) n_j\right) d\Gamma \\ & - \varepsilon^2 \int_\Gamma \left(\delta \bar{e}_{ij} R^{s-}_{ijprkl} \bar{e}_{kl,x_r} + \delta \bar{\sigma}_{ij} C^0_{ijmn} R^{s+}_{mnprst} C^0_{stkl} \bar{\sigma}_{kl,x_r}\right) n_p d\Gamma \end{aligned} \tag{25}$$

where Ω and Γ denote the domain of macrostructure and its boundary defined by outward normal vector $\boldsymbol{n}$, respectively; Γ_σ corresponds to the boundary where traction $f_i = \overline{\sigma}_{ij} n_j$ is prescribed. Note that equation (23) coincides with the Hu-Washizu principle in dynamics when ε approaches to zero.

Equation (23) follows from

$$\begin{cases} \int_\Omega \left(\delta U_i \rho_0 \ddot{U}_i + e_{xij}(\delta \boldsymbol{U}) \overline{\sigma}_{ij} + e_{xij}(\delta \boldsymbol{U}) \varepsilon^2 \rho_0 E_{ijkl} e_{xkl}(\ddot{\boldsymbol{U}}) \right) d\Omega \\ \qquad - \int_{\Gamma_\sigma} \delta U_i \varepsilon^2 \rho_0 E_{ijkl} e_{xkl}(\ddot{\boldsymbol{U}}) n_j d\Gamma = \int_{\Gamma_\sigma} \delta U_i f_i d\Gamma \\ \int_\Omega \left(\delta \overline{e}_{ij} D^0_{ijkl} \overline{e}_{kl} - \delta \overline{e}_{ij,x_r} \varepsilon^2 R^{s-}_{ijprkl} \overline{e}_{kl,x_p} - \delta \overline{e}_{ij} \overline{\sigma}_{ij} \right) d\Omega \\ \qquad + \int_\Gamma \delta \overline{e}_{ij} \varepsilon^2 R^{s-}_{ijprkl} \overline{e}_{kl,x_p} n_r d\Gamma = 0 \\ \int_\Omega \left(\delta \overline{\sigma}_{ij} e_{xij}(\boldsymbol{U}) - \delta \overline{\sigma}_{ij} \overline{e}_{ij} - \delta \overline{\sigma}_{ij,x_r} \varepsilon^2 C^0_{ijmn} R^{s+}_{mnprkl} C^0_{klst} \overline{\sigma}_{st,x_p} \right) d\Omega \\ \qquad + \int_\Gamma \delta \overline{\sigma}_{ij} \varepsilon^2 C^0_{ijmn} R^{s+}_{mnprkl} C^0_{klst} \overline{\sigma}_{st,x_p} n_r d\Gamma = 0 \end{cases} \tag{26}$$

which can be transferred into the weak form of equation (15) by taking integration by parts:

$$\begin{cases} \int_\Omega \delta U_i \left(\rho_0 \ddot{U}_i - \overline{\sigma}_{ij} + \varepsilon^2 \rho_0 E_{ijkl} e_{xkl}(\ddot{\boldsymbol{U}}) \right)_{,x_j} d\Omega = 0 \\ \int_\Omega \delta \overline{e}_{ij} \left(-\overline{\sigma}_{ij} + D^0_{ijkl} \overline{e}_{kl} + \varepsilon^2 R^{s-}_{ijprkl} \overline{e}_{kl,x_p x_r} \right) d\Omega = 0 \\ \int_\Omega \delta \overline{\sigma}_{ij} \left(-\overline{e}_{ij} + e_{xij}(\boldsymbol{U}) + \varepsilon^2 C^0_{ijmn} R^{s+}_{mnprkl} C^0_{klst} \overline{\sigma}_{st,x_p x_r} \right) d\Omega = 0 \end{cases} \tag{27}$$

Note that all boundary conditions in equation (23) can be neglected in case there is no reflection from the boundaries. To resolve the boundary layers boundary-matching scheme is required 7, 10.

3.1 Finite Element Discretization

The following matrix notation is employed for the finite element discretization.

$$\begin{cases} [U_1 \ U_2]^T = \boldsymbol{N}_{Ue} \boldsymbol{U}_e & , [e_{x11}(U) \ e_{x22}(U) \ 2e_{x12}(U)]^T = \boldsymbol{B}_{Ue} \boldsymbol{U}_e \\ [\overline{\sigma}_{11} \ \overline{\sigma}_{22} \ \overline{\sigma}_{12}]^T = \boldsymbol{N}_{\overline{\sigma}e} \overline{\boldsymbol{\sigma}}_e & , [\overline{\sigma}_{11,x_1} \ \overline{\sigma}_{11,x_2} \ \overline{\sigma}_{22,x_1} \ \overline{\sigma}_{22,x_2} \ \overline{\sigma}_{12,x_1} \ \overline{\sigma}_{12,x_2}]^T = \boldsymbol{B}_{\overline{\sigma}e} \overline{\boldsymbol{\sigma}}_e \\ [\overline{e}_{11} \ \overline{e}_{22} \ 2\overline{e}_{12}]^T = \boldsymbol{N}_{\overline{e}e} \overline{\boldsymbol{e}}_e & , [\overline{e}_{11,x_1} \ \overline{e}_{11,x_2} \ \overline{e}_{22,x_1} \ \overline{e}_{22,x_2} \ 2\overline{e}_{12,x_1} \ 2\overline{e}_{12,x_2}]^T = \boldsymbol{B}_{\overline{e}e} \overline{\boldsymbol{e}}_e \end{cases} \tag{28}$$

where the subscript e denotes the element number; $\boldsymbol{N}_{Ue}$ and $\boldsymbol{B}_{Ue}$ are the shape functions and the strain-displacement matrices, respectively.

Excluding the $O(\varepsilon^2)$ boundary terms the stabilized nonlocal equation (15) is given as

$$\sum_{e=1}^{nelm} \boldsymbol{M}_e \begin{Bmatrix} \ddot{\boldsymbol{U}} \\ \ddot{\overline{\boldsymbol{e}}} \\ \ddot{\overline{\boldsymbol{\sigma}}} \end{Bmatrix} + \sum_{e=1}^{nelm} \boldsymbol{K}_e \begin{Bmatrix} \boldsymbol{U} \\ \overline{\boldsymbol{e}} \\ \overline{\boldsymbol{\sigma}} \end{Bmatrix} = \begin{Bmatrix} \boldsymbol{f} \\ \boldsymbol{0} \\ \boldsymbol{0} \end{Bmatrix} \tag{29}$$

where,

$$\boldsymbol{M}_e = \begin{bmatrix} \boldsymbol{M}_{UU_e} & \boldsymbol{0} & \boldsymbol{0} \\ \boldsymbol{0} & \boldsymbol{0} & \boldsymbol{0} \\ \boldsymbol{0} & \boldsymbol{0} & \boldsymbol{0} \end{bmatrix} = \int_{\Omega_e} \begin{bmatrix} \boldsymbol{N}^T_{Ue} \rho \boldsymbol{N}_{Ue} + \varepsilon^2 \boldsymbol{B}^T_{Ue} \rho \boldsymbol{E} \boldsymbol{B}_{Ue} & \boldsymbol{0} & \boldsymbol{0} \\ \boldsymbol{0} & \boldsymbol{0} & \boldsymbol{0} \\ \boldsymbol{0} & \boldsymbol{0} & \boldsymbol{0} \end{bmatrix} d\Omega \tag{30}$$

$$\boldsymbol{K}_e = \begin{bmatrix} \mathbf{0} & \mathbf{0} & \boldsymbol{K}_{U\bar{\sigma}_e} \\ \mathbf{0} & \boldsymbol{K}_{\bar{e}\bar{e}_e} & \boldsymbol{K}_{\bar{e}\bar{\sigma}_e} \\ \boldsymbol{K}_{U\bar{\sigma}_e}^T & \boldsymbol{K}_{\bar{e}\bar{\sigma}_e}^T & \boldsymbol{K}_{\bar{\sigma}\bar{\sigma}_e} \end{bmatrix} = \int_{\Omega_e} \begin{bmatrix} \mathbf{0} & \mathbf{0} & \boldsymbol{B}_{Ue}^T \boldsymbol{N}_{\bar{\sigma}e} \\ \mathbf{0} & \boldsymbol{N}_{\bar{e}e}^T \boldsymbol{D}^0 \boldsymbol{N}_{\bar{e}e} - \varepsilon^2 \boldsymbol{B}_{\bar{e}e}^T \boldsymbol{R}^{s-} \boldsymbol{B}_{\bar{e}e} & -\boldsymbol{N}_{\bar{e}e}^T \boldsymbol{N}_{\bar{\sigma}e} \\ \boldsymbol{N}_{\bar{\sigma}e}^T \boldsymbol{B}_{Ue} & -\boldsymbol{N}_{\bar{\sigma}e}^T \boldsymbol{N}_{\bar{e}e} & -\varepsilon^2 \boldsymbol{B}_{\bar{\sigma}e}^T \boldsymbol{C}^0 \boldsymbol{R}^{s+} \boldsymbol{C}^0 \boldsymbol{B}_{\bar{\sigma}e} \end{bmatrix} d\Omega \quad (31)$$

Static condensation of the assumed nonlocal stresses and strains gives:

$$\boldsymbol{M}_{UU}\{\ddot{\boldsymbol{U}}\} + \tilde{\boldsymbol{K}}_{UU}\{\boldsymbol{U}\} = \{\boldsymbol{f}\} \quad (32)$$

where

$$\tilde{\boldsymbol{K}}_{UU} = \boldsymbol{K}_{U\bar{\sigma}}\left(-\boldsymbol{K}_{\bar{\sigma}\bar{\sigma}} + \boldsymbol{K}_{\bar{e}\bar{\sigma}}^T \boldsymbol{K}_{\bar{e}\bar{e}}^{-1} \boldsymbol{K}_{\bar{e}\bar{\sigma}}\right)^{-1} \boldsymbol{K}_{U\bar{\sigma}}^T \quad (33)$$

$$\boldsymbol{M}_{UU} = \sum_{e=1}^{nelm} \boldsymbol{M}_{UU_e} \quad , \boldsymbol{K}_{U\bar{\sigma}} = \sum_{e=1}^{nelm} \boldsymbol{K}_{U\bar{\sigma}_e} \quad , \boldsymbol{K}_{\bar{e}\bar{e}} = \sum_{e=1}^{nelm} \boldsymbol{K}_{\bar{e}\bar{e}_e} \quad , \boldsymbol{K}_{\bar{e}\bar{\sigma}} = \sum_{e=1}^{nelm} \boldsymbol{K}_{\bar{e}\bar{\sigma}_e} \quad , \boldsymbol{K}_{\bar{\sigma}\bar{\sigma}} = \sum_{e=1}^{nelm} \boldsymbol{K}_{\bar{\sigma}\bar{\sigma}_e} \quad (34)$$

Since $\boldsymbol{R}^{s-}$ and $\boldsymbol{R}^{s+}$ are semi-negative and semi-positive definite, respectively, $-\boldsymbol{K}_{\bar{\sigma}\bar{\sigma}}$ and $\boldsymbol{K}_{\bar{e}\bar{e}}^{-1}$ are semi-positive and positive definite, respectively. Hence, $-\boldsymbol{K}_{\bar{\sigma}\bar{\sigma}} + \boldsymbol{K}_{\bar{e}\bar{\sigma}}^T \boldsymbol{K}_{\bar{e}\bar{e}}^{-1} \boldsymbol{K}_{\bar{e}\bar{\sigma}}$ is positive and $\tilde{\boldsymbol{K}}_{UU}$ is semi-positive definite provided that the number of displacement degrees-of-freedom is larger than that of the assumed stresses. Thus the discretized approximation (32) is unconditionally stable in dynamics. Note that if only two-field principle were employed (see Peerlings et al.6), the discretized system might be unstable due to the indefinite character of $\boldsymbol{R}^s$.

4 Numerical Examples

To validate the proposed stabilized nonlocal model we consider plane harmonic and transient response problems with different microscopic and macroscopic configurations.

4.1 Macroscopically isotropic medium

As the first example, let us consider the macroscopically isotropic microstructure shown in Figure 1. Young modulus, Poisson's ratio, and density are given as E_1=1GPa, ν_1=0.2, ρ_1=$10^3 kg/m^3$ for material 1 and E_2=50GPa, ν_2=0.2, ρ_2=$10^3 kg/m^3$ for material 2. The cell domain is discretized by 60x104 square-shaped finite elements with four-node bilinear interpolation. The left edge of the macrostructure is fixed, while the right edge is subjected to the distributed impact load in the form of one sine-like function in the horizontal or vertical direction:

$$q(t) = \begin{cases} a_0(t - T/2)\{t(t-T)\}^4 & 0 \le t \le T \\ 0 & t > T \end{cases} \qquad N/mm^2 \quad (35)$$

where a_0 is scaled so that $-1 \le q(t) \le 1$ and T denotes the load duration. The macrostructure is discretized by square-shaped finite elements with eight-node serendipity interpolation for the nonlocal displacement U_i and four-node bilinear interpolations for both the assumed nonlocal strains $\bar{e}_{ij}$ and the assumed nonlocal stresses $\bar{\sigma}_{ij}$. The size of the square-shaped elements is 5mm which corresponds to the half-length of the cell. Newmark β method (β=0, γ=1/2) is employed for time integration.
The impact load (35) with duration time T=70μs, which produces Gauss function like wave of about 135mm for the P-wave and about 82mm for the S-wave, is applied in the horizontal and vertical direction. Figure 2 shows the time history of the vertical nonlocal displacement at the center of the macro-domain for the horizontal load. The reference solution was obtained by numerically solving the

heterogeneous system. Good agreement between the stabilized nonlocal model and the reference solutions can be observed, while the solutions obtained by the classical $O(1)$ homogenization shows significant discrepancies. Moreover, it can be seen that the solutions obtained using the proposed nonlocal model and the previously developed 5 macroscopically isotropic nonlocal model (16) are almost identical.

4.2 Stratified Medium

Consider the periodic unit cell shown in Figure 3, corresponding to the horizontally stratified medium composed of two dissimilar materials. The Young modulus, Poisson's ratio, and density are the same as in the previous example. The cell domain is discretized by 30^2 square-shaped finite elements with four-node bilinear interpolation. Stratified medium is one of the configurations known to cause strong dispersion. Waves traveling in the vertical direction can be modeled as one-dimensional problem, whereas waves in horizontal direction have to be modeled in two dimensions.

4.2.1 Plane Harmonic Wave Analysis

To analyze the stability properties of the original nonlocal model (11) and the proposed nonlocal model (15) we consider the plane harmonic wave analysis. Figure 4 plots the relation between the wave number and the phase velocity for the wave propagating in the horizontal direction. Exact solution 1213(for details see Appendix) is also plotted for comparison. In Figure 4, two lines for each solution correspond to the lowest symmetric and asymmetric deformation modes. It can be seen that the original nonlocal model (11) is unstable (phase velocity becomes imaginary) for the wave number k=20*2π/m corresponding to the wavelength which is 5 times of that of the unit cell. This instability shows up only in the case of the macroscopic domain discretized with the mesh size comparable to that of the unit cell. On the other hand, the phase velocity for the stabilized nonlocal model (15) is real for all wave numbers, but the solution becomes inaccurate for wave numbers larger than k=20*2π/m. The stabilization proposed here (15) can be interpreted as a high-frequency filter.

4.2.2 Transient Wave Analysis in stratified semi-infinite domain

The semi-infinite macro-domain shown in Figure 5 is considered to validate the stability and the accuracy of the proposed model (15). The infinite domain in the vertical direction is modeled by periodic boundary conditions. The length of the domain in the horizontal direction is 1000*mm*. The boundary on the left is fixed, while the right edge is subjected to the impact load (35). Finite element interpolations are the same as in the previous example.
The impact load (35) with duration time T=50μs, which produces Gauss function like wave of about 260*mm* for the P-wave and about 45*mm* for the S-wave, is applied in the horizontal and vertical directions, respectively. Figures 6 and 7 show the time history of the horizontal nonlocal displacement at the center of the macro-domain for the horizontal load and the time history of the vertical displacement for the vertical load, respectively. Reference solutions were obtained by solving numerically the heterogeneous system. Good agreement between the proposed stabilized nonlocal model and the reference solutions can be seen, while the solutions obtained by the classical $O(1)$ homogenization and by the previous macroscopically-isotropic nonlocal model (16) err badly.

4.2.3 Transient Wave Analysis in stratified finite domain

Consider a square macro-domain of 260*mm* in each direction as shown in Figure 8. The vertical boundary conditions are the same as in the previous example. The horizontal boundaries are stress-free. Three unit cells denoted as A, B and C in Figure 8 are considered. From the macroscopic description point of view the three cells are identical, but their reflections characteristics from the boundary are different. Figures 9 and 10 show the time history of the horizontal nonlocal displacement at the center of the macro-domain for the horizontal load with duration time of T=50μs and the time history of the vertical displacement for the vertical load, respectively. The solutions obtained by the proposed stabilized nonlocal model are generally in reasonable agreement with the reference solutions, while the solutions obtained by the classical $O(1)$ homogenization show significant deviations. Figure 9 shows that as the time increases and the waves are reflected from the boundaries the proposed stabilized nonlocal model becomes inaccurate.

4.3 Transient wave analysis in semi-infinite domain with checker-board microstructure

Consider a semi-infinite macro-domain shown in Figure 5 with the checker-board microstructure shown in Figure 11. The load and the boundary conditions are the same as in Section 4.2.2. Figures 12 and 13 show the time history of the horizontal nonlocal displacement at the center of the macro-domain for the horizontal load and the time history of the vertical displacement for the vertical load, respectively. Good agreement between the proposed stabilized nonlocal model and the reference solutions can be seen, while the solutions obtained by the classical $O(1)$ homogenization and by the previous model (16) show significant discrepancies in particular for the vertical load in Figure 13.

5 Concluding Remarks

A stabilized nonlocal model for dispersive wave motion in heterogeneous media has been developed. The model has been validated for problems on infinite and semi-infinite domains. The model incorporates periodic boundary conditions between the unit cells including boundary layers and therefore does not properly resolve wave reflections from the boundaries. Various boundary layer approaches and appropriate matching schemes are currently being investigated. An additional drawback of the method stems from the C^0-approximation of the assumed nonlocal strains and stresses. Various Discontinuous Galerkin formulations are currently being tested to allow for static condensations of these fields at the element level.
An interesting observation is that the mass matrix (see equation (30)), consists of the classical mass matrix (consistent or lumped), as well as a dispersion-induced mass, which depends on the microstructural properties and the relative size of the microstructure compared to the component size. For low strain rates the second term has been found to be negligible. Since the dispersion fourth order tensor E_{ijkl} is positive definite (see equation (8)) the added mass term gives rise to lower deformation energy absorption at high strain rates recently observed in the crash experiments[11].

Acknowledgment

This work was supported by the Sandia National Laboratories under Contract DE-AL04-94AL8500, the Office of Naval Research through grant number N00014-97-1-0687, and the Japan Society for the Promotion of Science under contract number Heisei 11-nendo 06542.

References

1. Sanchez-Palencia E. (1980) *Non-homogeneous Media and Vibration Theory*, Springer, Berlin

Formatted: Bullets and Numbering

2. Benssousan A., Lions J. L., and Papanicoulau G. (1978) *Asymptotic Analysis for Periodic Structures*, North Holland, Amsterdam
3. Bakhvalov N.S. and Panasenko G.P.(1989) *Homogenization: Averaging Processes in Periodic Media*, Kluwer, Dordrecht
4. Fish J. and Chen W. (2001) *Higher-order homogenization of initial/boundary-value problem*, ASCE J. Eng. Mech., Vol. 127, No.12, pp.1223-1230
5. Fish J., Chen W., and Nagai G. (2002) *Nonlocal dispersive model for wave propagation in heterogeneous media Part1 &2*, Int. J. Num. Meth. Eng. Vol. 54, pp. 331-363
6. Peerlings R.H.J., Borst R. de, Brekelmans W.A.M. and Vree J.H.P. de (1996) *Some observations on localization in non-local and gradient damage models*, Eur. J. Mech. A/Solids, 15, pp.937-953
7. Muhlhaus H. B. and Aifantis E. C. (1991) *A variational principle for gradient plasticity*, Int. J. Solids Structures Vol. 28, No. 7, pp.845-857
8. Boutin C. and Auriault J. L. (1990) *Dynamic behavior of porous media saturated by a viscoelastic fluid. Application to bituminous concretes*, Int. J. Engng. Sci., 28(11), pp.1157-1181.
9. Boutin C. and Auriault J.L. (1993) *Rayleigh scattering in elastic composite materials*, Int. J. Engng. Sci. Vol.31 No.12, pp.1669-1689
10. Boutin C. (1996) *Microstructural effects in elastic composites*, Int. J. Solids Struct. 33(7), pp.1023-1051.
11. M.E. Botkin, "Crash Prediction of Composite Structures" private communications, May, 2003.
12. Sun C. T., Achenbach J. D. and Herrmann G. (1968) *Continuum theory for a laminated medium*, J. Appl. Mech., 35, pp. 467-475
13. Sun C. T., Achenbach J. D. and G. Herrmann (1968) *Time-harmonic waves in a stratified medium propagating in the direction of the layering*, J. Appl. Mech., 35, pp. 408-411

Formatted: Bullets and Numbering

Appendix

Consider an infinitely stratified medium, in which dissimilar isotropic materials are stacked alternatively. As shown in Figure A1, the local coordinates of each stack is defined so that x_2=0 is aligned along the centerline with x_1 being same for all layers. λ and μ are Lamé's constants and ρ is mass density. The subscript m denotes material phase.

With the notation of $i=\sqrt{-1}$, phase velocity c, and wave number k, for matrix domain, the displacement of the plane harmonic wave propagating in the horizontal direction can be expressed as

$$\boldsymbol{u}_m(\boldsymbol{x}) = \boldsymbol{A}_m(x_{m2})\exp[ik(x_1 - ct)] \tag{A1}$$

The displacements can be further decomposed as follows:

$$\begin{aligned} &\boldsymbol{u}_m = \boldsymbol{u}_{ml} + \boldsymbol{u}_{mt} \\ &\text{rot}\,\boldsymbol{u}_{ml} = 0, \quad \text{div}\,\boldsymbol{u}_{mt} = 0 \end{aligned} \tag{A2}$$

Considering equation (A2), each element of $\boldsymbol{u}$ can be expressed as

$$\begin{aligned} u_{m1} &= (A_{ml1} + A_{mt1})\exp[ik(x_1 - ct)] \\ u_{m2} &= (A_{ml2} + A_{ml2})\exp[ik(x_1 - ct)] \end{aligned} \tag{A3}$$

where,

$$\begin{aligned} A_{ml1} &= \quad a_{ml}\cos(kq_m x_{m2}) + ib_{ml}\sin(kq_m x_{m2}) \\ A_{mt1} &= -s_m\{b_{mt}\cos(ks_m x_{m2}) + ia_{mt}\sin(ks_m x_{m2})\} \\ A_{ml2} &= \quad q_m\{b_{ml}\cos(kq_m x_{m2}) + ia_{ml}\sin(kq_m x_{m2})\} \\ A_{mt2} &= \quad a_{mt}\cos(ks_m x_{m2}) + ib_{mt}\sin(ks_m x_{m2}) \end{aligned} \tag{A4}$$

$$\begin{aligned} q_m &= \sqrt{c^2/c_{ml}^2 - 1}\,, \quad c_{ml}^2 = (\lambda_m + 2\mu_m)/\rho_m \\ s_m &= \sqrt{c^2/c_{mt}^2 - 1}\,, \quad c_{mt}^2 = \mu_m/\rho_m \end{aligned} \tag{A5}$$

Stress components related to tractions at the interface are given as

$$\begin{aligned} \sigma_{m22} &= ik\mu_m\{(s_m^2 - 1)A_{ml1} - 2A_{mt1}\}\exp[ik(x_1 - ct)] \\ \sigma_{m12} &= ik\mu_m\{2A_{ml2} - (s_m^2 - 1)A_{mt2}\}\exp[ik(x_1 - ct)] \end{aligned} \tag{A6}$$

Similarly, displacements and stresses in the fiber domain can be obtained by replacing the subscript m to f.

Continuity conditions of displacements and tractions on each interface, yields the following eight equations:

$$\begin{aligned} u_{m1}(x_{m2} = h_m) &= u_{f1}(x_{f2} = -h_f) & u_{m1}(x_{m2} = -h_m) &= u_{f1}(x_{f2} = h_f) \\ u_{m2}(x_{m2} = h_m) &= u_{f2}(x_{f2} = -h_f)\,, & u_{m2}(x_{m2} = -h_m) &= u_{f2}(x_{f2} = h_f) \\ \sigma_{m22}(x_{m2} = h_m) &= \sigma_{f22}(x_{f2} = -h_f) & \sigma_{m22}(x_{m2} = -h_m) &= \sigma_{f22}(x_{f2} = h_f) \\ \sigma_{m22}(x_{m2} = h_m) &= \sigma_{f22}(x_{f2} = -h_f) & \sigma_{m22}(x_{m2} = -h_m) &= \sigma_{f22}(x_{f2} = h_f) \end{aligned} \tag{A7}$$

resulting in

$$\begin{bmatrix} \mathbf{G}_s & \mathbf{0} \\ \mathbf{0} & \mathbf{1} \end{bmatrix} \begin{bmatrix} \mathbf{1} & \mathbf{0} \\ \mathbf{0} & \mathbf{G}_a \end{bmatrix} \begin{Bmatrix} \mathbf{A}_s \\ \mathbf{A}_a \end{Bmatrix} = \mathbf{0} \tag{A8}$$

where **1** denotes 4x4 unit matrix and

$$\mathbf{G}_s = \begin{bmatrix} \cos(kq_m h_m) & -s_m\cos(ks_m h_m) & -\cos(kq_f h_f) & -s_f\cos(ks_f h_f) \\ iq_m\sin(kq_m h_m) & i\sin(ks_m h_m) & iq_f\sin(kq_f h_f) & i\sin(ks_f h_f) \\ i\mu_m k(s_m^2-1)\cos(kq_m h_m) & 2i\mu_m ks_m\cos(ks_m h_m) & -i\mu_f k(s_f^2-1)\cos(kq_f h_f) & -2i\mu_f ks_f\sin(ks_f h_f) \\ -2\mu_m kq_m\sin(kq_m h_m) & \mu_m k(s_m^2-1)\sin(ks_m h_m) & -2\mu_f kq_f\sin(kq_f h_f) & \mu_f k(s_f^2-1)\sin(ks_f h_f) \end{bmatrix}$$

$$\mathbf{G}_a = \begin{bmatrix} i\sin(kq_m h_m) & -i\,s_m\sin(ks_m h_m) & i\sin(kq_f h_f) & i\,s_f\sin(ks_f h_f) \\ q_m\cos(kq_m h_m) & \cos(ks_m h_m) & -q_f\cos(kq_f h_f) & -\cos(ks_f h_f) \\ -\mu_m k(s_m^2-1)\sin(kq_m h_m) & -2\mu_m ks_m\sin(ks_m h_m) & -\mu_f k(s_f^2-1)\sin(kq_f h_f) & -2\mu_f ks_f\sin(ks_f h_f) \\ 2i\mu_m kq_m\cos(kq_m h_m) & -i\mu_m k(s_m^2-1)\cos(ks_m h_m) & -2i\mu_f kq_f\cos(kq_f h_f) & i\mu_f k(s_f^2-1)\cos(ks_f h_f) \end{bmatrix}$$

$$\begin{aligned} \mathbf{A}_s &= [a_{tf}\ \ b_{lf}\ \ a_{tm}\ \ b_{lm}]^T \\ \mathbf{A}_a &= [a_{lf}\ \ b_{tf}\ \ a_{lm}\ \ b_{tm}]^T \end{aligned} \tag{A9}$$

For the nontrivial solution of equation (A8) to exist the determinant of the matrix must vanish. Hence, we have

$$\det(\mathbf{G}_s)\det(\mathbf{G}_a) = 0 \tag{A10}$$

Note that from equations (A8) and (A3), the deformation has been decomposed into symmetric and asymmetric modes. The det($\mathbf{G}_s$)=0 and det($\mathbf{G}_a$)=0 are the corresponding conditions, respectively.

Equation (A10) must be solved numerically with respect to the phase velocity c for each wave number k.

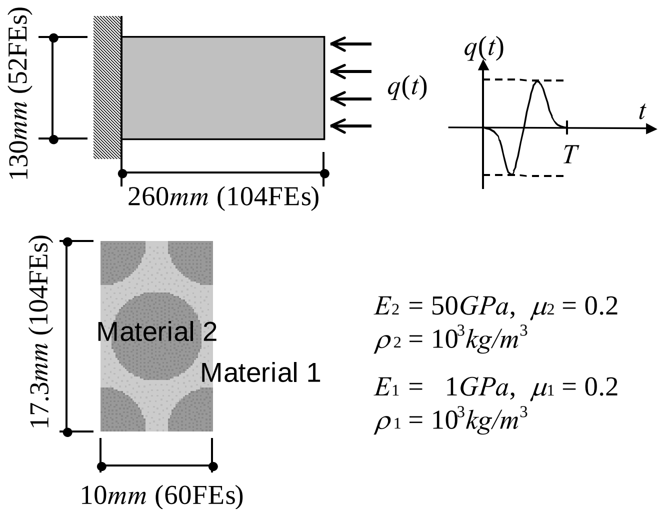

Figure 1: Configuration of macroscopically isotropic medium and macrostructure

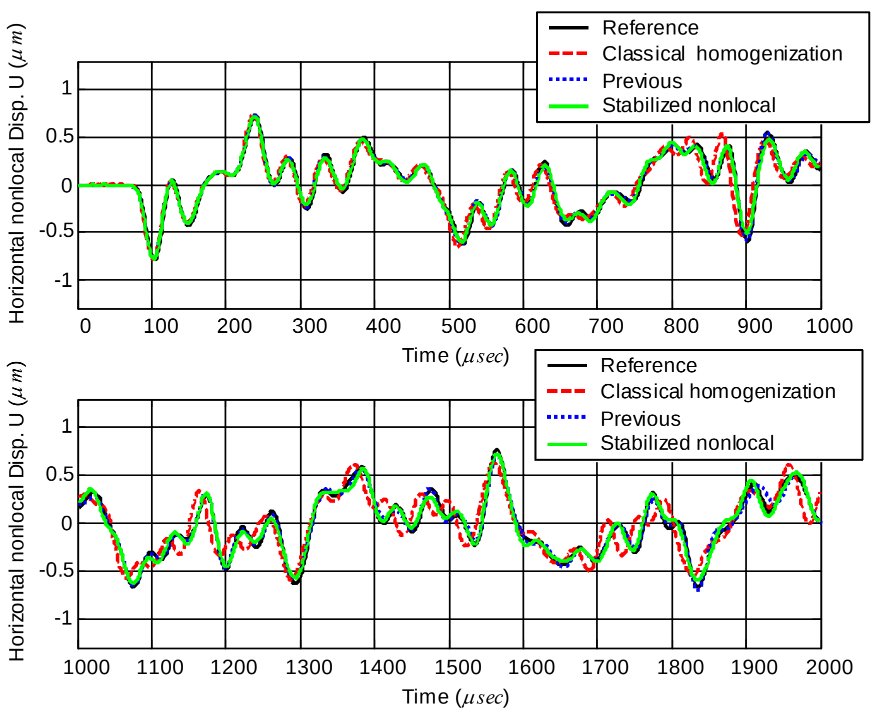

Figure 2: Horizontal nonlocal displacement at center

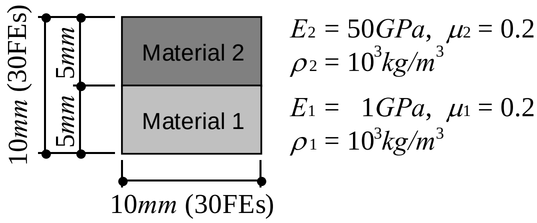

Figure 3: Configuration of microscopic unit cell of stratified medium

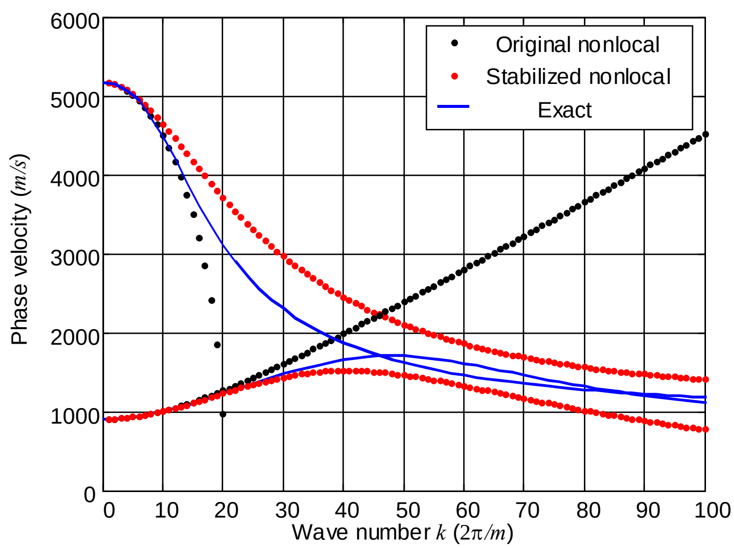

Figure 4: Phase velocity spectrum of stratified medium

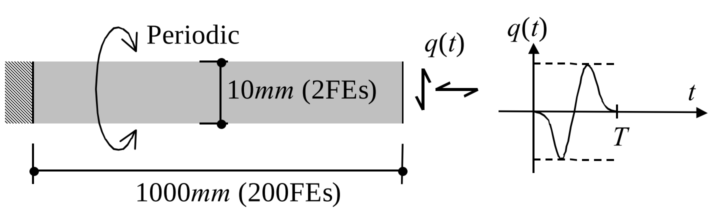

Figure 5: Configuration of periodic macrostructure

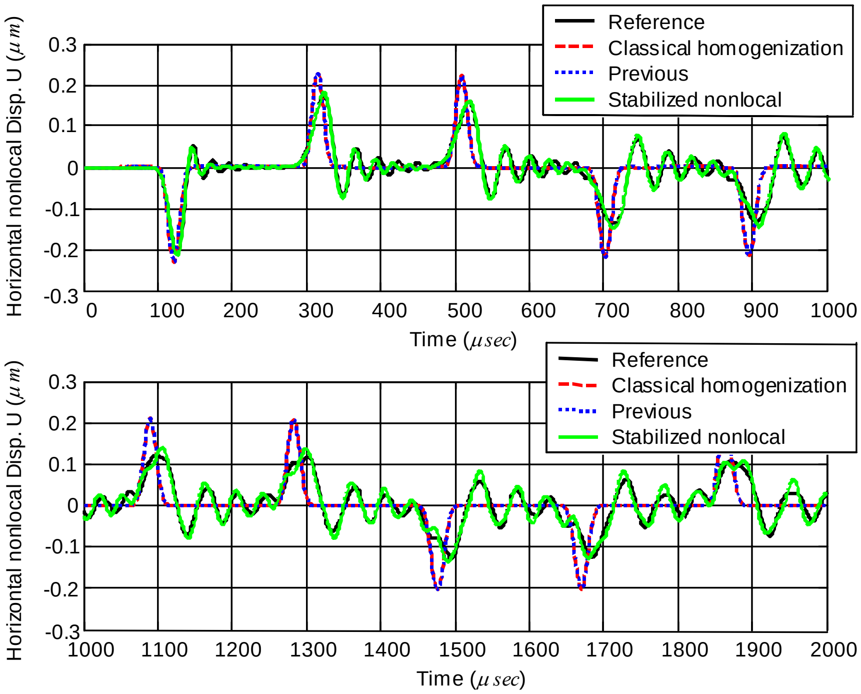

Figure 6: Horizontal nonlocal displacement at center for horizontal load

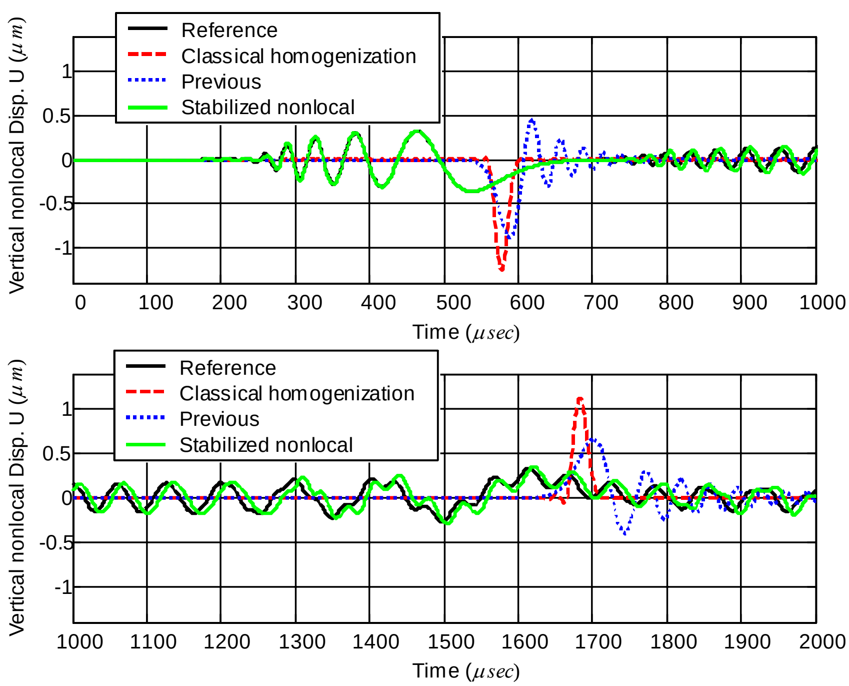

Figure 7: Vertical nonlocal displacement at center for vertical load

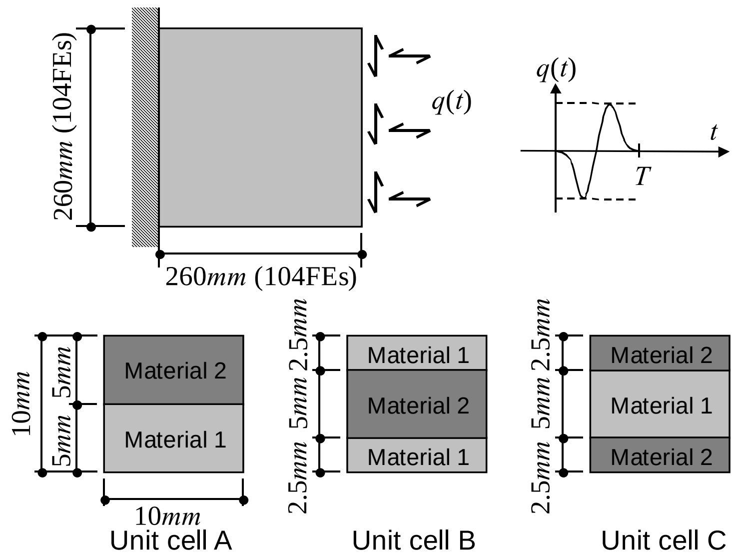

Figure 8: Configuration of macrostructure and microstructures

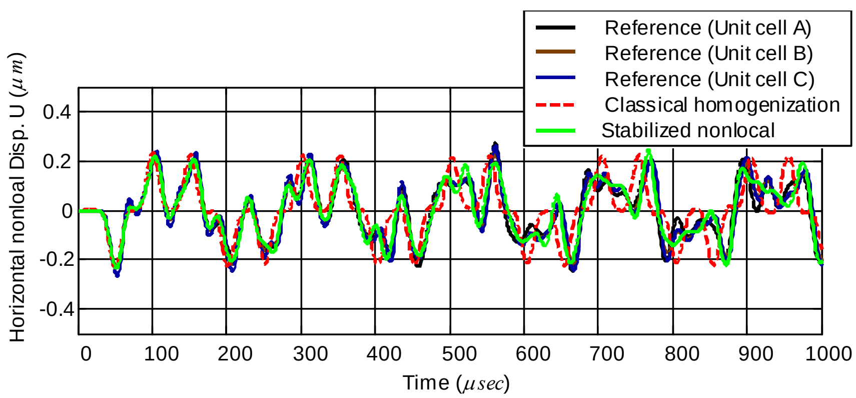

Figure 9: Horizontal nonlocal displacement at center for horizontal load

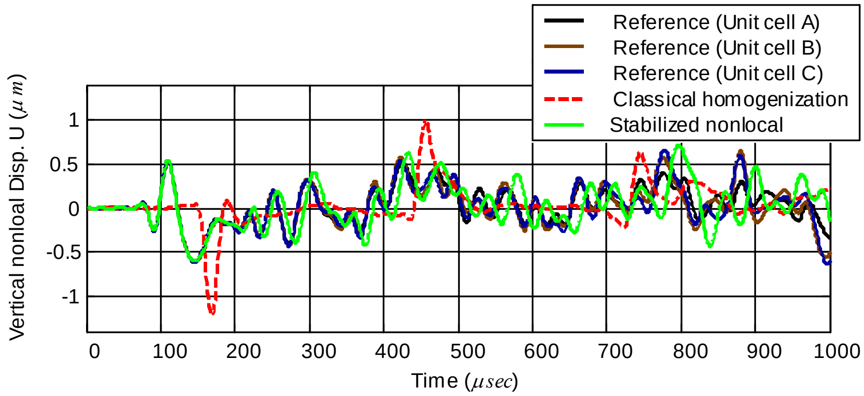

Figure 10: Vertical nonlocal displacement at center for vertical load

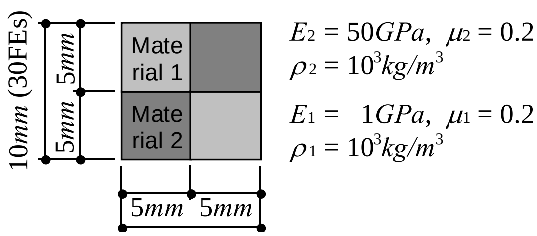

Figure 11: Configuration of checker-board microstructure

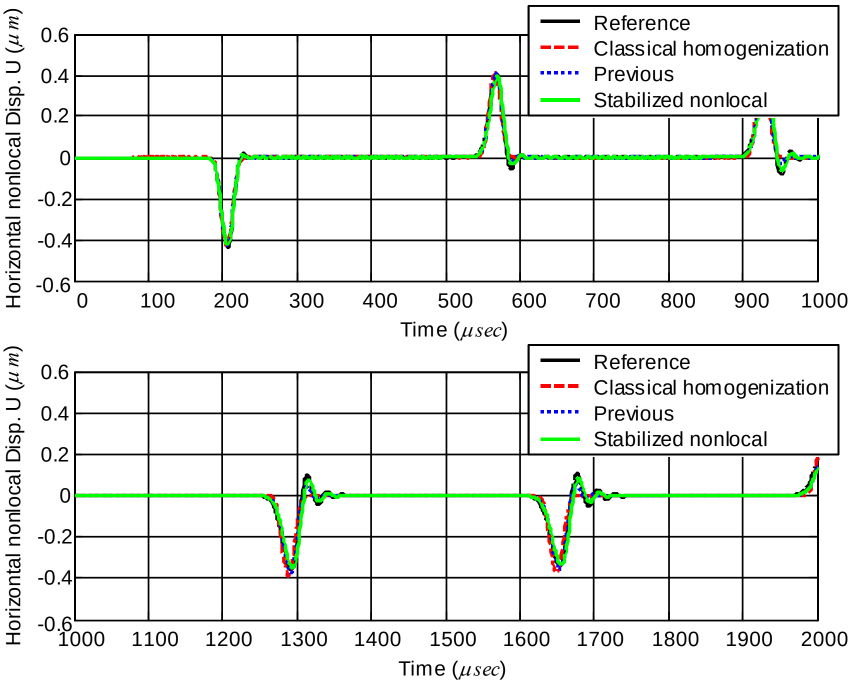

Figure 12: Horizontal nonlocal displacement at center for horizontal load

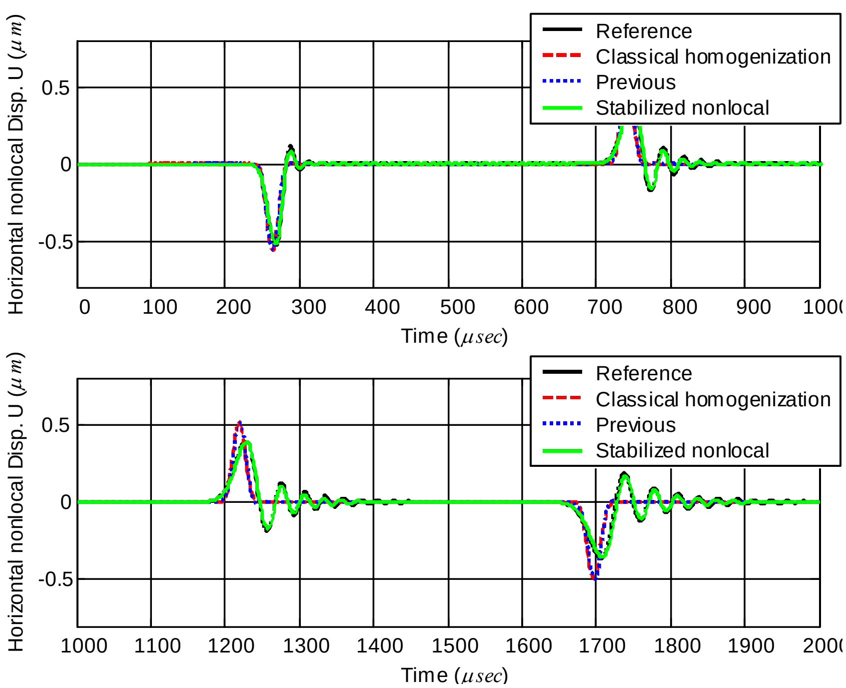

Figure 13: Vertical nonlocal displacement at center for vertical load

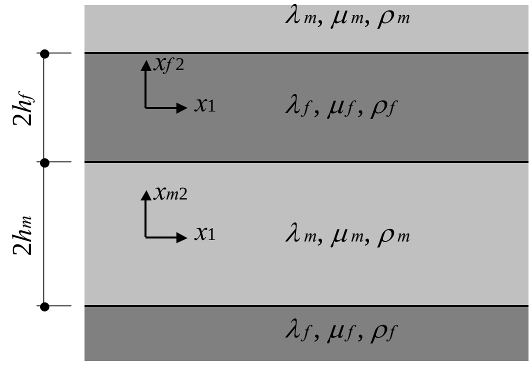

Figure A1: Horizontally stratified medium